

Novel Polypyridyl Ruthenium(II) Complexes Containing Oxalamidines as Ligands

M. Ruben[§], S. Rau[§], A. Skirl[§], K. Krause[§], H. Görls[§], D. Walther^{§*}, J. G. Vos^{&*}

[§] Friedrich-Schiller-Universität Jena, Institut für Anorganische und Analytische Chemie, August-Bebel-Strasse 2, 07743 Jena, Germany

[&] Inorganic Chemistry Research Centre, School of Chemical Sciences, Dublin City University, Dublin 9, Ireland

Received:

Abstract

The complexes [Ru(bpy)₂(H₂TPOA)](PF₆)₂ · 4H₂O, (**1**); [Ru(Me-bpy)₂(H₂TPOA)](PF₆)₂ · 2H₂O, (**2**); [Ru(bpy)₂(H₂TTOA)](PF₆)₂ · 2H₂O, (**3**); [Ru(Me-bpy)₂(H₂TTOA)](PF₆)₂ · 2H₂O, (**4**) and {[Ru(bpy)₂]₂(TPOA)}(PF₆)₂ · 2H₂O, (**5**) (where bpy is 2,2'-bipyridine; Me-bpy is 4,4'-dimethyl-2,2'-bipyridine; H₂TPOA is N, N', N'', N'''- tetraphenylloxalamidine; H₂TTOA is N, N', N'', N'''- tetratolylloxalamidine) have been synthesized and characterized by ¹H-NMR, FAB-MS, infrared spectroscopy and elemental analysis. The X-ray investigation shows the coordination of the still protonated oxalamidine moiety via the 1,2-diimine unit. The dimeric compound (**5**) could be separated in its diastereoisomers (**5'**) and (**5''**) by repeated recrystallisation. The diastereomeric forms exhibit different ¹H-NMR spectra and slightly shifted electronic spectra. Compared with the model compound [Ru(bpy)₃]²⁺, the absorption maxima of (**1**)–(**5**) are shifted to lower energies. The mononuclear complexes show Ru(III/II)-couples at about 0.9 V vs SCE, while for the dinuclear complex two well defined metal based redox couples are observed at 0.45 and 0.65 V indicating substantial interaction between the two metal centres.

keywords: ruthenium complexes, oxalamidines, diastereomer separation, redox properties

1. Introduction

Oligonuclear polypyridyl Ru(II) complexes are currently being investigated in detail because of their rich electrochemical and photophysical properties which render them very attractive systems for modeling electron and energy transfer processes [1], which are known to play a crucial role in biological processes such as respiration, photosynthesis and oxydative DNA cleavage [2].

In most of the compounds described so far the Ru(II) metal center is bound to aromatic and polyaromatic pyridyl compounds containing 1,2-diimine units [3]. Less attention has been paid to compounds containing ligands in which the chelating 1,2-diimine unit is not part of an aromatic system [4] [5]. In this contribution novel of ruthenium polypyridyl complexes containing nonaromatic 1,2-diimines are further considered and we report our studies on mono- and dinuclear Ru(II) complexes containing N, N', N'', N'''' - tetraaryloxalamidines (aryl = phenyl: **H₂TPOA**; aryl = tolyl: **H₂TTOA**). (For structures of these ligands see Figure 1)

((insert here: Figure 1))

The purpose of these investigations is to study the effect that these non-aromatic diimine ligands have on the absorption spectra and the electrochemical properties of ruthenium polypyridyl moieties. Of interest is also to determine the coordination mode of the ligands. Since oxalamidines can be deprotonated [9] several coordination modes are possible for this type of ligand. The acid-base properties of the ligands can in principle also be used to tune the electronic properties of the ruthenium polypyridyl complexes obtained. The coordination chemistry of these ligands with complex fragments such as Mo(CO)₄; BR₂ (R=Me); and Cu(I)L [6 - 8] has already been reported.

2. Experimental Section

Materials: H₂TPOA and H₂TTOA were prepared according literature procedures [10].

RuCl₃.xH₂O was purchased from Strem Chemical and used without further purification. 2,2'-bipyridine and 4,4'-dimethyl-2,2'-bipyridine were obtained from Aldrich.

Instrumentation and Measurements: ¹H-NMR spectra were obtained on a Bruker AC 200 MHz spectrometer and all spectra were referenced to TMS or deuteriated solvent as an internal standard. UV-Vis spectra were recorded on a Shimadzu UV 3100 spectrometer using Teflon stoppered quartz cells having a path length of 1 cm. FAB-MS data were obtained on a Finnigan MAT SSQ 710 instrument using 2,4-dimethoxybenzylalcohol as matrix. Studies of the acid base properties were carried out in a 50/50 % (v:v) mixture of acetonitrile and Britton-Robinson buffer (0.04 M H₃BO₃; 0.04 M H₃PO₃; 0.04 M CH₃COOH). This mixture was used for all measurements and the pH was measured directly with an EDT Microprocessor pH-meter calibrated with standard buffers of pH 4.0 and pH 7.0. The pK_a constants were obtained from the absorption spectra with the aid of a diagram ΔAbs% vs pH. The electrochemical cell was a conventional three compartment cell. The reference electrode was a saturated calomel electrode and the working electrode was 3 mm diameter teflon shrouded glassy carbon electrode and a platinum gauze was used as the counter electrode. A solution of 0.1 M tetraethylammonium perchlorate (TEAP) in acetonitrile was used as electrolyte in all measurements. Cyclic voltammetry was carried out on a CH-instruments model 660 Electrochemical Workstation interfaced to an Elonex PC466 personal computer. Analytical HPLC experiments were carried out using a Waters HPLC system, consisting of a model 501 pump, a 20 μl injector loop, a Partisil SCX radial PAK cartridge mounted in a radial compression Z module and a Waters 990 photodiode array detector. The system was controlled by a NEC APC III computer. The detection wavelength was 290 nm. The mobile phase used was 90:10 CH₃CN:H₂O containing 0.1 M LiClO₄. Elemental analysis on C,H and

N were carried out at the Microanalytical Laboratory of the University College Dublin and at the Friedrich-Schiller-University Jena.

Preparations: A typical protocol for preparation of compounds **(1)**-**(4)** is as follows (here described for $[\text{Ru}(\text{bpy})_2(\text{H}_2\text{TPOA})](\text{PF}_6)_2 \cdot 4\text{H}_2\text{O}$, **(1)**): 0.416 g (0.8 mmol) of $\text{Ru}(\text{bpy})_2\text{Cl}_2 \cdot 2\text{H}_2\text{O}$ were dissolved in 50 ml ethanol/water (95:5 v/v%) and subsequently 0.390 g (1.0 mmol) of H_2TPOA was added. The mixture was refluxed for 24 h, during which the colour changed from violet to deep red. After cooling to room temperature the solution was evaporated to dryness. The resulting residue was redissolved in a small amount of acetonitrile and purified using column chromatography (Al_2O_3 ; acetonitrile/toluene). The brick red main band was collected and the complex precipitated by adding an excess of aqueous NH_4PF_6 . The precipitate was isolated, washed with diethylether and dried under vacuum. Alternatively the pure compounds can be also obtained by fractional crystallisation from acetone/water.

$[\text{Ru}(\text{bpy})_2(\text{H}_2\text{TPOA})](\text{PF}_6)_2 \cdot 4\text{H}_2\text{O}$, **(1)**, yield: 84 %; **$^1\text{H-NMR}$** [D_6 -DMSO, δ , ppm, 20°C]: 10.02 (s, NH, 2H); 9.23 (d, H^6 , 2H), 8.42 (d, H^3 , 2H); 8.24 (t, H^4 , 2H); 8.12 (d, H^3 , 2H); 8.05 (t, H^5 , 2H); 7.71 (t, H^4 , 2H); 7.47 (d, H^6 , 2H), 7.19 (t, H^5 , 2H); 6.96 (t, H_{arom} , 4H); 6.83 (d, H_{arom} , 4H); 6.78 (t, H_{arom} , 2H); 6.56; 6.49; 5.31 (dynamisystem, H_{arom} , 10H); **FAB-MS** [dmbsa, m/z]: 949 ($[\text{M}^+] - \text{PF}_6^-$); 804 ($[\text{M}^+] - 2\text{PF}_6^-$); **IR** [nujol; ν , cm^{-1}]: 3382 (m, NH); 3075 (w, arom. C-H); 1595 (s, C=N); 1448 (s, C=C), 842, 557 (s, PF_6^-); **UV-VIS** [acetonitrile, λ_{MLCT} , nm]: 469 ($\epsilon = 13938 \text{ l cm}^{-1} \text{ mol}^{-1}$); **CV** [acetonitrile, 0,1 M TEAP vs SCE, $E_{\text{Ru(III/II),V}}$]: 0.94; *Anal.*: calc. C, 48.89; H, 3.75; N, 9.92; found: C, 48.49; H, 3.95; N, 9.88.

$[\text{Ru}(\text{Me-bpy})_2(\text{H}_2\text{TPOA})](\text{PF}_6)_2 \cdot 2\text{H}_2\text{O}$, **(2)**, yield: 75 %; **$^1\text{H-NMR}$** [D_6 -DMSO, δ , ppm, 20°C]: 9.98 (s, NH, 2H); 9.32 (d, H^6 , 2H), 8.42 (d, H^3 , 2H); 8.11 (d, H^3 , 2H); 7.96 (t, H^5 , 2H); 7.54 (d, H^6 , 2H), 7.14 (t, H^5 , 2H); 7.00 (t, H_{arom} , 2H); 6.99 (t, H_{arom} , 4H); 6.79 (d, H_{arom} , 4H); 6.57; 6.45; 5.37 (dynamic system, H_{arom} , 10H); 2.69 (s, CH_3 , 6H); 2.34 (s, CH_3 , 6H);

FAB-MS [dmbs, m/z]: 1005 ($[M^+ - PF_6^-]$); 859 ($[M^+ - 2PF_6^- - H^+]$); **IR** [nujol; ν , cm^{-1}]: 3367 (m, NH); 3060 (w, arom. C-H); 2924 (w, C-H); 1619 (s, C=N); 1450 (s, C=C), 845, 558 (s, PF_6^-); **UV-VIS** [acetonitrile, λ_{MLCT} , nm]: 476 ($\epsilon = 11728 \text{ l cm}^{-1} \text{ mol}^{-1}$); **CV**[acetonitrile, 0,1 M TEAP vs SCE, $E_{Ru(III/II), V}$]: 0.90; *Anal.*: calc.: C, 52.20; H, 4.03; N 9.78;; found: C, 51.88; H, 4.92; N, 8.74.

[Ru(bpy)₂(H₂TTOA)](PF₆)₂ · 2H₂O, (3), yield: 72%. **¹H-NMR** [D₆-DMSO, δ , ppm, 20°C] : 9.95 (s, NH, 2H); 9.35 (d, H⁶, 2H), 8.36 (d, H³, 2H); 8.09 (m, H⁴ u. H⁵, 4H); 7.98 (t, H⁵, 2H); 7.60 (t, H⁴, 2H); 7.43 (d, H⁶, 2H), 7.08 (t, H⁵, 2H); 6.57 (dd, H_{arom}, 8H); 6.08; 5.49; (dynamic System, H_{arom}, 8H); 2.00 (s, CH₃, 6H); 1.80 (s, CH₃, 6H); **FAB-MS** [dmbs, m/z]: 1006 ($[M^+ - PF_6^- + H^+]$); 860 ($[M^+ - 2PF_6^-]$); **IR** [nujol; ν , cm^{-1}]: 3366 (m, NH); 2923 (w, C-H); 1593 (s, C=N); 1463 (s, C=C), 841, 557 (s, PF_6^-); **CV** [acetonitrile, 0,1 M TEAP vs SCE, $E_{Ru(III/II), V}$]: 0.96; **UV-VIS** [acetonitrile, λ_{MLCT} , nm]: 472 ($\epsilon = 11274 \text{ l cm}^{-1} \text{ mol}^{-1}$); *Anal.*: calc. C, 50.42; H, 4.25; N, 9.44; found : C, 50.91; H, 4.94; N, 8.66.

[Ru(Me-bpy)₂(H₂TTOA)](PF₆)₂ · 2H₂O, (4); yield: 45 %. **¹H-NMR** [D₆-DMSO, δ , ppm, 20°C] : 9.56 (s, NH, 2H); 8.96 (d, H⁶, 2H), 8.23 (d, H³, 2H); 7.98 (d, H³, 2H); 7.85 (t, H⁵, 2H); 7.18 (d, H⁶, 2H), 7.05 (t, H⁵, 2H); 6.80 (dd, H_{arom}, 8H); 6.40 (dynamic System, m, H_{arom}, 8H); 2.62 (s, CH₃, 6H); 2.26 (s, CH₃, 6H); 2.06 (s, CH₃, 6H); 1.93 (s, CH₃, 6H); **FAB-MS** [dmbs, m/z]: 1061 ($[M^+ - PF_6^- + H^+]$); 1004 ($[M^+ - 2PF_6^- - 3F^-]$); 915 ($[M^+ - 2PF_6^- - H^+]$); **IR** [nujol; ν , cm^{-1}]: 3371 (m, NH); 3029 (w, arom. C-H); 2924 (w, C-H); 1618 (s, C=N); 1450 (s, C=C), 845, 558 (s, PF_6^-); **CV** [acetonitrile, 0,1 M TEAP vs SCE, $E_{Ru(III/II), V}$]: 0.87; **UV-VIS** [acetonitrile, λ_{MLCT} , nm]: 478 ($\epsilon = 13983 \text{ l cm}^{-1} \text{ mol}^{-1}$); *Anal.*: calc. C, 53.78; H, 4.51; N 9.29;; found : C, 54.60; H 4.68; N, 8.76.

Preparation of {[Ru(bpy)₂]₂(TPOA)}(PF₆)₂ · 2H₂O (5): 195 mg (0.5 mmol) of TPOA were dissolved in 60 ml ethanol/water (50:50 v/v %). An excess of 0.671 g (0.8mmol) of Ru(bpy)₂Cl₂·2H₂O was added and the resulting solution was refluxed for 8 hours. The

reaction mixture was treated with an excess of aqueous NH_4PF_6 . The precipitate was redissolved in acetone/water and pure and mixed fractions of the meso-($\Delta\Delta$)-compound and the unresolved ($\Delta\Delta/\Lambda\Lambda$) enantiomeric pair (**5'** and **5''**) could be isolated subsequently by fractional crystallisation. Yield: 1.3 g (84 %) of (**5'** and **5''**).

(5'): $^1\text{H-NMR}$ [D_6 -DMSO, δ , ppm, 20°C]: 8.78 (d, H^6 , 4H); 8.71 (d, H^3 , 4H); 8.56 (d, H^3 , 4H); 8.18 (t, H^4 , 4H); 7.77 (t, H^4 , 4H); 7.69 (t, H^5 , 4H); 7.30 (d, H^6 , 4H); 7.14 (t, H^5 , 4H); 6.68 (t, H_{arom} , 4H); 6.53 (t, H_{arom} , 8H); 5.97 (d, H_{arom} , 8H); **IR** [nujol; ν , cm^{-1}]: 3036(w, arom. C-H); 1592 (s, C=N); 1489, 1444 (s, C=C); 842, 557 (PF_6^-); **UV-VIS** [acetonitrile, λ_{MLCT} , nm]: 520; **CV** [acetonitrile, 0.1 M TEAP vs SCE, $E_{\text{Ru(III/II)}}$, V]: 0.45; 0.64; *Anal. calc.* C, 51.43; H, 3.66; N, 10.91; found: C, 52.23; H, 3.42; N, 10.90.

(5''): $^1\text{H-NMR}$ [D_6 -DMSO, δ , ppm, 20°C]: 9.09 (d, H^6 , 4H); 8.90 (d, H^3 , 4H); 8.68 (d, H^3 , 4H); 8.41 (t, H^4 , 4H); 8.12 (t, H^5 , 4H); 7.80 (t, H^4 , 4H); 7.29 (d, H^6 , 4H); 7.13 (t, H^5 , 4H); 6.41 (t, H_{arom} , 4H); 6.09 (t, H_{arom} , 8H); 5.70 (d, H_{arom} , 8H); **IR** [nujol; ν , cm^{-1}]: 3036 (w, arom. C-H); 1592 (s, C=N); 1489, 1444 (s, C=C); 842, 557 (PF_6^-); **UV-VIS** [acetonitrile, λ_{MLCT} , nm]: 526; **CV** [acetonitrile, 0.1 M TEAP vs SCE, $E_{\text{Ru(III/II)}}$, V]: 0.46; 0.65; *Anal. calc.:* C, 51.43; H, 3.66; N, 10.91;; found : C, 52.87; H, 3.98; N, 10.84.

Crystal structure determination of $[(\text{bpy})_2\text{Ru}(\text{H}_2\text{TPOA})](\text{PF}_6)_2 \cdot 4\text{H}_2\text{O}$ (**1**)

X-ray diffraction was carried out on a Nonius Kappa CCD diffractometer, using graphite-monochromated Mo- $\text{K}\alpha$ radiation and ϕ -scan technique ($\Delta\phi = 1^\circ$, scan-range 180° , time/frame = 30s) at 20°C . Data were corrected for Lorentz and polarization effects, but not for absorption [13].

The structure was solved by direct methods (SHELXS [14]) and refined by full-matrix least squares techniques against F^2 (SHELXL-93 [15]). The hydrogen atoms (without the water molecules) were located by difference Fourier synthesis and refined isotropically. All

nonhydrogen atoms were refined anisotropically. XP (SIEMENS Analytical X-ray Instruments, Inc.) was used for structure representations.

3. Results and discussion

Synthesis and Structure of Mononuclear Complexes (1) - (4)

The synthesis of ruthenium oxalamidine compounds was accomplished using standard methods. The nuclearity of resulting complexes could be governed by controlling the metal to ligand ratio (See Figure 2). Nevertheless, in the case of the mononuclear compounds **(1)**- **(4)** some dimer formation could not be prevented and a subsequently cleaning by column chromatography was necessary. The ^1H -NMR spectra do exhibit the expected pattern of the bpy protons in a C_2 -symmetric $\text{Ru}(\text{bpy})_2$ environment. All protons of the bipyridine ligands could be unambiguously attributed by ^1H - ^1H - COSY-experiments.

((insert here Figure 2))

The signals that can be attributed to the aromatic substituents of the coordinated oxalamidine ligands are found at higher field than the bipyridine protons. At room temperature, only half of the expected aromatic signals for **(1)**-**(4)** are well resolved peaks (See for example compound **(3)** in Figure 3). Thus, compound **(3)** shows for half of the tolyl protons at room temperature one well resolved AA`BB` spin system, while the other half is observed as a broadened signal at about 6.0 ppm. Upon heating this signal becomes the expected AA`MM` spin system at 5.49 and 6.08 ppm. This dynamic process is most likely explained by hindered rotation of the aryl substituents on the oxalamidine ligands. Interestingly, this behaviour is not observed in the binuclear compound **(5)** (*vide infra*). This can be explained by enhanced crowding around the tetraphenylloxalamidine bridging ligand, not allowing for any rotation of the aryl substituents around the C-N bond.

((insert here **Figure 3**))

An important aspect of this study is establishing the coordination mode of the oxalamidine ligand. The tetradentate nature of these ligands allows different coordination modes (see figure 4) and possible deprotonation of the ligands also needs to be considered.

((insert here **Figure 4**))

The presence of protonated secondary amino functions in the mononuclear complexes **(1)** -**(4)** was established from $^1\text{H-NMR}$ measurements, by infrared spectroscopy and by elemental analysis. This protonation behaviour is contrary to that of triazole ligands, where a secondary N-H function is being deprotonated upon coordination [11]. The composition of compounds **(1)** - **(4)** was further confirmed by FAB-MS, in which the complexes exhibit characteristic losses of the only electrostatically bound PF_6^- -anions rendering the cationic complex fragment as the most intense signal (see experimental part).

In order to establish the coordination mode of the ligand, the X-ray structure of **(1)** was determined. Some relevant distances and angles are given in Table 1. As in solution, **(1)** exhibits C_2 -symmetry in the solid state. The result of the X-ray-investigations depicted in Figure 5 demonstrates clearly octahedral coordination of the Ru(II)-ion by two bipyridine ligands and by one H_2TPOA ligand. The latter ligand is coordinated via the 1,2-diimine unit. The secondary amines are clearly protonated. The C-N(H)-bond length ($d_{\text{C-N}} = 1.355(5) \text{ \AA}$) reveals partial double bond character probably due to delocalisation of the double bond in the amidine system, but the 1,2-diimine unit is clearly defined by its significantly shorter C-N-distance ($d_{\text{C-N}} = 1.294(4) \text{ \AA}$). This allows one to draw the unambiguous conclusion, that the tetraphenylloxalamidine is coordinated via its 1,2-diimine system (**C** in Figure 4). It is

worth emphasizing that H₂TPOA is bound there in its s-cis configuration while the free ligand exists in crystal only as s-trans conformer [12].

((insert here:Figure 5))

The Ru-N(bpy)-distances ($d_{\text{Ru-N}} = 2.049(3) \text{ \AA} - 2.053(3) \text{ \AA}$) are in the typical range of other members of the Ru(bpy)₂(LL)-class [2], while the Ru-N(oxalamidine) distances are slightly elongated ($d_{\text{Ru-N}} = 2.081(3) \text{ \AA}$) indicating the weaker back bonding character of the oxalamidine ligand or maybe a steric hindrance by the phenyl groups. Interestingly the Ru-N distance in the, also neutral, dihydrazone type ligands are significantly shorter at 2.01 Å [4]. The N-Ru-N „bite“ angles show the anticipated values ($\alpha = 78.7(1)^\circ$) for the bipyridines, while the „bite“ angle of the oxalamidine do not exceed $\alpha = 75.4(2)^\circ$ due to easier pinching of the nonrigid oxalamidine system.

((insert here: Table 1))

In addition, the X-ray investigations reveal intermolecular interactions. In the crystalline state compound (**1**) forms a polymeric chain of alternating ordered complex cations whereby the cations are interconnected by interaction of each N-H-function with a planar ring consisting of four water molecules (see Figure 6). The distance $d_{\text{N(H)-O}} = 2.957(6) \text{ \AA}$ is in the typical range of H-bonding distances, while the distances between the oxygen atoms within in the planar water four ring are 2.778(5) Å and 2.957(5) Å. Thus, highly ordered solvent molecules create a supramolecular arrangement in the crystal .

((insert here: Figure 6))

It is worth mentioning that the position of the outwards directed phenyl rings seems to suggest a π - π -interaction. But compared with literature values [16], the distance of $d_{\text{phenyl-phenyl}} = 3.78 \text{ \AA}$ in the phenyl stacks indicates rather only simple crystal packing effects than π - π -interaction as reason for this particular arrangement.

***Synthesis and Structure of the Dinuclear Compound* $\{[\text{Ru}(\text{bpy})_2]_2(\text{TPOA})\}(\text{PF}_6)_2 \cdot 2\text{H}_2\text{O}$,
(5)**

The use of more as twofold excess of $\text{Ru}(\text{bpy})_2$ -precursor yields the dinuclear compound (5) in good yield. HPLC measurements indicate the presence of two compounds with a peak area of 50:50 %. It was possible to separate these by recrystallisation in acetone/water (60/40 v/v%). Elemental analysis yielded identical composition for both compounds and was indicative of a deprotonation of the tetraphenyloxalamidine ligand in both cases. The ^1H -spectra of the two fractions were recorded in d_6 -DMSO and are depicted in Figure 7. The spectra are only slightly different and exhibit a quite simple pattern with only one set of aromatic phenyl signals as expected for a high symmetrical complex. All peaks could be assigned unequivocally with help of COSY experiments. No broad peaks as in the mononuclear compounds appear in the spectra and the phenyl rings of the TPOA^{2-} bridging ligand show only one well-resolved set of two triplets and one doublet. This suggests that in the dinuclear compound the aryl rings are not free to rotate. The protons of the bipyridine ligands show the usual shifts and pattern.

((insert here Figure 7))

On the basis of these observations it seems reasonable to assume that the two fractions are optical isomers (5') and (5''). The presence of stereoisomers is related to the well-known stereochemical problem of linking two metal ions with helical chirality by a bridging ligand

[17]. This causes the emergence of one meso-form ($\Delta\Lambda$) and one enantiomeric pair with $\Delta\Delta$ and $\Lambda\Lambda$ configuration. The two isolated diastereomeric isomers (**5'**) and (**5''**) should correspond to the meso- $(\Delta\Lambda)$ -compound and to the unresolved $(\Delta\Delta/\Lambda\Lambda)$ enantiomeric pair (enantiomers are undistinguishable in $^1\text{H-NMR}$ -spectroscopy) [18] but with the data available it was not possible to assign the absolute configuration of (**5'**) and (**5''**).

Absorption Spectra

The absorption spectra of compound (**1**)-(**5**) were recorded in methanol/ethanol and show the typical features for members of the polypyridyl ruthenium (II) class. The results are summarised in Table 3. The most significant feature of these spectra is a strong band in the visible range due to $d\pi-\pi^*$ -MLCT transitions [19].

((insert Table 2))

In comparison to the model compound $[\text{Ru}(\text{bpy})_3]^{2+}$ ($\lambda_{\text{MLCT}} = 452 \text{ nm}$), the MLCT bands of the oxalamidine complexes exhibit a shift to lower wavenumbers. Therefore, it can be suggested that the investigated oxalamidines possess stronger σ -donor and weaker π -acceptor properties than bipyridine. The presence of methylsubstituents in (**2**) and (**4**) has only a minor influence on the absorption maxima. The MLCT-maximum of the dinuclear compound is observed at lower energy than in the monomeric compounds. This reflects the deprotonation of the bridging ligand and it is indicative of the stronger σ -donor and weakened π -acceptor properties of the deprotonated bridge.

The possibility of tuning of the absorption spectra of the compounds (**1**) – (**4**) by changing the acidity of the solution was investigated. Thus, Figure 8 shows the absorption spectra of compound (**1**) in the range from $\text{pH} = 3.08$ to 12.05 . In this range only one set of isobestic

points is found. The MLCT-band around $\lambda = 470$ nm collapses gradually upon deprotonation and two new bands appear. The emerging band at $\lambda = 505$ nm can be assigned to a MLCT transition in the deprotonated complex. The deprotonated tetraphenylloxalamidine ligand should act as stronger σ -donor and increasing electron density around the metal shifts the maximum of the MLCT-band to higher wavelengths. The band at $\lambda = 380$ nm might be correspond to an additional MLCT band to either bpy or to H₂TPOA.

From the absorption spectra it was possible to determine the pK_a values for (1) – (4) (See Table 2). The pK_a is relatively insensitive to substitution changes on both the bpy ligand and the oxalamidines. Only one protonation step could be observed in the range measured for all complexes. This might suggest that both N-H functions are deprotonated at the same time or that the second deprotonation is outside the range measured.

((insert figure 8))

The two diastereomers (5') and (5'') show slightly different absorption spectra (see figure 9). Potential differences in the electronic behaviour of diastereomeric and enantiomeric isomers of polypyridyl ruthenium(II) complexes were recently subject of several investigations [20, 21]. Multinuclear ruthenium polypyridyl complexes will normally contain a manifold of diastereomers and these studies are aimed at determining whether optical isomers have significantly different photophysical properties. That is a rather important problem, because constructing antenna systems from Ru-bipyridyl units demands the very strict control of the photophysical properties of such light absorbing devices.

Surprisingly, the measurement of compounds (1)-(5) do not show any emission. Even chilling down to 77 K in various solvents and extended change of the pH-value did not render the expected emission. This is a unexpected result, because the appearance of a emission from a long living ³MLCT state is to be seen as one of intrinsic characteristic for polypyridyl-Ru(II)

compounds. One possible explanation might be that the electron occupies an oxalamidine π^* -orbital instead of a bipy π^* -orbital in the excited state. Thus, the inappropriateness of the oxalamidine π^* -orbitals to deliver a long living excited state could explain the absence of emission. This assumption might be supported by the first reduction potentials for compounds **(1)** - **(4)** which are irreversible, in contrast to those of polypyridyl-Ru(II) complexes.

((insert Figure 9))

Electrochemistry

The Ru(III)/(II) potentials for the PF₆-salts in 0.1 M solution of tetra-n-butylammonium perchlorate in acetonitrile versus saturated calomel electrode are summarised in Table 3. In comparison with [Ru(bpy)₃]²⁺ (E_{III/II} = 1.23 V vs SCE) all redox Ru(III/II) couples of the mononuclear complexes **(1)** - **(4)** are shifted to more negative potentials (E_{III/II} = 0.96 V - 0.87 V), in agreement with an increased electron density around the ruthenium ion caused by the better σ -donor properties of the oxalamidine ligands. Methyl substitution on the bipyridine ligands pushes the Ru(III/II) couples to somewhat more negative potentials consistent with the results of before described absorption measurements. Substitution at the oxalamidine does affect the oxidation couple hardly. The oxidation potentials for the two isomers of the dimeric compound **(5)** differ only slightly. The oxidation of the dinuclear complexes results in two one electron single waves, which are in both isomers separated by 190 mV. Using this value the comproportionation constant K_{com} for **(5)** was calculated following the relationship (at T=298 K) [22]

$$K_{\text{com}} = \exp\{\Delta E(\text{mV})/25.69\} = 1.63 \cdot 10^3$$

This value points to a substantial electronic interaction between the two metal centres. The oxidation of the first centre causes an increase in the charge of the complex and therefore the second oxidation occurs at higher potential. In compound **(5)** the first oxidation couple occurs at $E_{\text{III/II}} = 0.45 - 0.46$ V exhibiting the strong σ -donor capability of the deprotonated bridging ligand. Thus, even the second oxidation occurs at more negative potential ($E_{\text{III/II}} = 0.64/0.65$ V) than the lowest of the mononuclear compounds, for which the oxidation potential is found at about 0.90 V. This is most likely explained by the double negative charge on the bridging ligand.

5. Conclusion

We have prepared series of novel mononuclear complexes of the type $[\text{Ru}(\text{bpy})_2(\text{LL})]^{2+}$ with $\text{LL} = \text{H}_2\text{TPOA}, \text{H}_2\text{TTOA}$ as members of a new class of non aromatic 1,2-diimine ligands in polypyridyl Ruthenium(II) chemistry. The structure of the mononuclear compounds was elucidated by $^1\text{H-NMR}$, FAB-MS and X-ray investigations. The coordination of the $\text{Ru}(\text{bpy})_2$ -moiety to the 1,2-diimine unit was assured unambiguously by X-ray structure determination of compound $[\text{Ru}(\text{bpy})_2(\text{H}_2\text{TPOA})](\text{PF}_6)_2 \cdot 4\text{H}_2\text{O}$, **(1)**. On supramolecular level, complex **(1)** forms chainlike structures, whereby the complex cations are interconnected via their N-H functions by four ordered water molecules. Surprisingly, the complexes **(1)**- **(5)** do not exhibit any emission under any condition. The dinuclear compound $\{[\text{Ru}(\text{bpy})_2]_2\text{TPOA}\}(\text{PF}_6)_2 \cdot 2\text{H}_2\text{O}$, **(5)** was prepared and structurally characterised. We succeeded in separating the two diastereomers by recrystallisation and could confirm small but significant differences in electronic spectra.

Finally we propose that since they possess potential for H-bonding and intercalation by π -stacking with biological substrates (e.g. DNA) the mononuclear complexes **(1)**- **(4)** can

become valuable building blocks in supramolecular architectures. Future research efforts will follow this line.

6. Supplementary material

Further details of the crystal investigations are available on requests from the Fachinformationszentrum Karlsruhe, Gesellschaft für wissenschaftlich – technische Information mbH, D-76344 Eggenstein-Leopoldshafen, on quoting the depository number CSD ###, the names of the authors, and the journal citation.

Acknowledgements

We would like to thank to Prof. U.-W. Grummt and Mrs. E. Backhaus for collaboration in some experiments and for measuring several spectra. This work was financially supported by the „Studienstiftung des deutschen Volkes“ by a doctoral scholarship for M.R. and S. R. and by “Deutsche Forschungsgemeinschaft” (SFB 436).

References

- [1] (a) J.-P. Collin, P. Gavina, P. Heitz, J.-P. Sauvage, *Eur. J. Inorg. Chem.* 1 (1998) 1.(b) A. Livoreil, J.-P. Sauvage, N. Armaroli, V. Balzani, L. Flamigni, B. Ventura, *J. Am. Chem. Soc.* 119 (1997) 12114. c) V. Balzani, A. Juris, M. Venturi, S. Campagna, S. Serroni, *Chem. Rev.* 96 (1996) 759.
- [2] (a) R.E. Holmlin, P.J. Dadliker, J.K. Barton, *Angew. Chem., Int. Ed. Engl.* 36 (1997) 2714. (b) A. Magnuson, Y. Frapart, M. Abrahamson, O. Horner, B. Åckermark, L. Sun, J.-J. Girerd, L. Hammarström, S. Styring, *J. Am. Chem. Soc.* 121 (1999) 89.
- [3] J.-P. Sauvage, J.-P. Collin, J.-C. Chambron, S. Guillerez, C. Coudret, V. Balzani, F. Barigelletti, L. DeCola, L. Flamigni, *Chem. Rev.* 94 (1994) 993.

- [4] J. A. Bolger, G. Ferguson, J. P. James, C. Long, P. McArdle, J. G. Vos, *J. Chem. Soc. Dalton Trans.* (1993) 1577.
- [5] A. Juris, V. Balzani, F. Barigelletti, S. Campagna, P. Belser, A. v. Zelewsky, *Coord. Chem. Rev.* 84 (1988) 85.
- [6] M. Döring, H. Görls, R. Beckert, *Z. Anorg. Allg. Chemie* 620 (1994) 551.
- [7] J. Trofimenko, *J. Am. Chem. Soc.* 89 (1967) 7014.
- [8] E. Papafil, A. Papafil, A. Kleinstein, I. Gabe, V. Macovei, *Analele Stiint. Univ. "Al. I. Cuza" Iasi, Sect. I* 10c(2) (1964) 115.
- [9] D. Lindauer, R. Beckert, M. Döring, P. Fehling, H. Goerls, *J. Prakt. Chem.* 337 (1995) 143.
- [10] K. Bauer, *Chem. Ber.* 40 (1907) 2655.
- [11] (a) R. Hage, J. G. Haasnoot, J. Reedijk, R. Wang, J. G. Vos, *Inorg. Chem.* 30 (1991) 3263. (b) R. Hage, *Coordination Chemistry Reviews* 111 (1991) 161.
- [12] S. Vorwerk, Diploma thesis (1992), Friedrich-Schiller-University Jena
- [13] Z. Otwinowski, W. Minor, „Processing of X-Ray Diffraction Data Collected in Oscillation Mode“, in *Methods in Enzymology, Vol. 276, Macromolecular Crystallography, Part A*, edited by C.W. Carter & R.M. Sweet, Academic Press, pp. 307-326.
- [14] G.M. Sheldrick, *Acta Crystallogr. Sect. A* 46 (1990) 467.
- [15] G.M. Sheldrick, *SHELXL-97*, University of Göttingen, Germany, (1993)
- [16] C. A. Hunter, J. K. M. Sanders, *J. Am. Chem. Soc.* 112 (1990) 5525.
- [17] A. von Zelewsky, *Chimia* 48 (1993) 331.
- [18] B. Testa, „Grundlagen der Organischen Stereochemie“, Verlag Chemie, Weinheim, (1983) pp.158
- [19] K. Kalanyanasundaram, „Photochemistry of Polypyridine and Porphyrin Complexes“, Academic Press, London, (1992)

- [20] (a) X. Hua, A. v. Zelewsky, *Inorganic Chem.* 30 (1991) 3796. (b) K. Wärnmark, J. Thomas, O. Heyke, J.-M. Lehn, *J. Chem. Soc., Chem. Commun.* (1994) 2075 (c) F.R. Keene, *Coord. Chem. Rev.* 166 (1997) 121. (d) F.R. Keene, *Chem. Soc. Rev.* 27 (1998) 185.
- [21] (a) S. Serroni, G. Denti, S. Campagna, M. Ciano, V. Balzani, *J. Am. Chem. Soc.* 114 (1992) 2944; (b) S. Serroni, G. Denti, S. Campagna, A. Juris, M. Ciano, V. Balzani, *Angew. Chem., Int. Ed. Engl.* 31 (1992) 1493; (c) T. J. Rutherford, O. Van Gijte; A. Kirsch-De Mesmaker, F. R. Keene, *Inorg. Chem.* 1997, 36, 4465.
- [22] G. Giuffrida, S. Campagna, *Coord. Chem. Rev.* 135/136 (1994) 517.

Capture of Figures

Figure 1: Structure of the ligands

Figure 2: Synthesis of mononuclear complexes (1) - (4) and dimeric complex (5)

Figure 3: $^1\text{H-NMR}$ spectra of $[(\text{bpy})_2\text{Ru}(\text{H}_2\text{TTOA})](\text{PF}_6)_2 \cdot 2\text{H}_2\text{O}$, (3), at 293 K and 383 K exhibiting the dynamic behaviour of the aromatic protons of the tetratolyloxalamidine

Figure 4: Possible coordination modes of the oxalamidine ligand towards the $\text{Ru}(\text{bpy})_2$ -moiety

Figure 5: Drawing of the X-ray structure of $[(\text{bpy})_2\text{Ru}(\text{H}_2\text{TPOA})](\text{PF}_6)_2 \cdot 4\text{H}_2\text{O}$, (1), (anions and solvent molecules are omitted for reasons of clarity)

Figure 6: Supramolecular structure of $[(\text{bpy})_2\text{Ru}(\text{H}_2\text{TPOA})](\text{PF}_6)_2 \cdot 4\text{H}_2\text{O}$, (1) (anions are omitted for reasons of clarity)

Figure 7: $^1\text{H-NMR}$ spectra of the two diastereomers ($5'$) (above) and ($5''$) (below) in D_6 -DMSO at 293 K

Figure 8: pH-dependence of the absorption spectra of $[\text{Ru}(\text{bpy})_2(\text{H}_2\text{TPOA})](\text{PF}_6)_2 \cdot 4\text{H}_2\text{O}$, (1) in the range from pH 3.08 to 12.05

Figure 9: UV-VIS spectra of compounds ($5'$) (---) and ($5''$) (-)

Table 1: Selected bond lengths (Å) and angles (°) for [Ru(bpy)₂(H₂TPOA)](PF₆)₂·4H₂O,**(1)**

Ru-N(4)	2.049(3)	N(4)-Ru-N(4A)	173.8(2)
Ru-N(3)	2.053(3)	N(4)-Ru-N(3A)	97.0(1)
Ru-N(1)	2.081(3)	N(4)-Ru-N(3)	78.7(1)
N(1)-C(1)	1.294(4)	N(3A)-Ru-N(3)	91.6(2)
N(2)-C(1)	1.355(5)	N(4)-Ru-N(1)	85.7(1)
C(1)-C(1A)	1.503(6)	N(4A)-Ru-N(1)	99.3(1)
N(2)-O(1)	2.957(6)	N(3A)-Ru-N(1)	171.9(1)
O(1)-O(2)	2.778(5)	N(3)-Ru-N(1)	96.5(1)
O(1)-O(2A)	2.862(5)	N(1)-Ru-N(1A)	75.4(2)

Table 2: Absorption maxima and electrochemical data of the complexes **(1)** - **(5)** in acetonitril; pK_a values for **(1)** – **(4)**

compound	λ_{MLCT} [nm]	ϵ [l cm ⁻¹ mol ⁻¹]	Ru(III/II) V	pK _a
[Ru(bpy) ₃] ²⁺ [5]	452	1.46 · 10 ⁴	1.26	-
[Ru(bpy) ₂ (H ₂ TPOA)] ²⁺ (1)	469	1.39 · 10 ⁴	0.94	9.19
[Ru(Me-bpy) ₂ (H ₂ TPOA)] ²⁺ (2)	476	1.17 · 10 ⁴	0.90	9.33
[Ru(bpy) ₂ (H ₂ TTOA)] ²⁺ (3)	472	1.12 · 10 ⁴	0.96	9.94
[Ru(Me-bpy) ₂ (H ₂ TTOA)] ²⁺ (4)	478	1.40 · 10 ⁴	0.87	10.15
{[Ru(bpy) ₂] ₂ (TPOA)} ²⁺ (5)				
(5')	520	(n. n.)	0.45/0.64	-
(5'')	526	(n. n.)	0.46/0.65	-

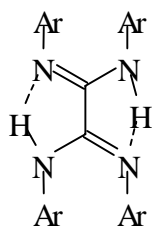
Annex:

Crystallographic data for [Ru(bpy)₂(H₂TPOA)](PF₆)₂ · 4H₂O, (1)

empiric Formula	C ₄₆ H ₃₈ F ₁₂ N ₈ P ₂ Ru * 4H ₂ O
formula weight [g mol ⁻¹]	1159.87
crystal size	
space group	C2/c
crystal size[mm]	0.20 x 0.20 x 0.10
crystal colour	red-brown
a (Å)	23.037(5)
b (Å)	12.739(3)
c (Å)	18.550(4)
β °	114.04(3)
temperature [K]	293
volume [Å ³]	4971(1)
Z	4
density (calc.) [g cm ⁻³]	1.550
Θ range for data collection [°]	3.10 to 23.26
Limiting indices	0 ≤ h ≤ 25, 0 ≤ k ≤ 14, -20 ≤ l ≤ 18
reflections collected	5951
R _{int}	0.034
independent reflections	3572
observed reflections [I > 2σ (I)]	3344
absorption coefficient [cm ⁻¹]	4.76
Parameters/restrains	461/12
Final R indices [I > 2σ (I)]	R ₁ =0.038 wR ₂ =0.095
R indices (all data)	R ₁ =0.055 wR ₂ =0.104
Goodness-of-fit F ²	1.009
Largest diff. Peak and hole [eÅ ⁻³]	0.556 and -0.450

List of Figures

[Figure 1]



Ar = Ph **H₂TPOA**
Ar = Tol **H₂TTOA**

[Figure 2]

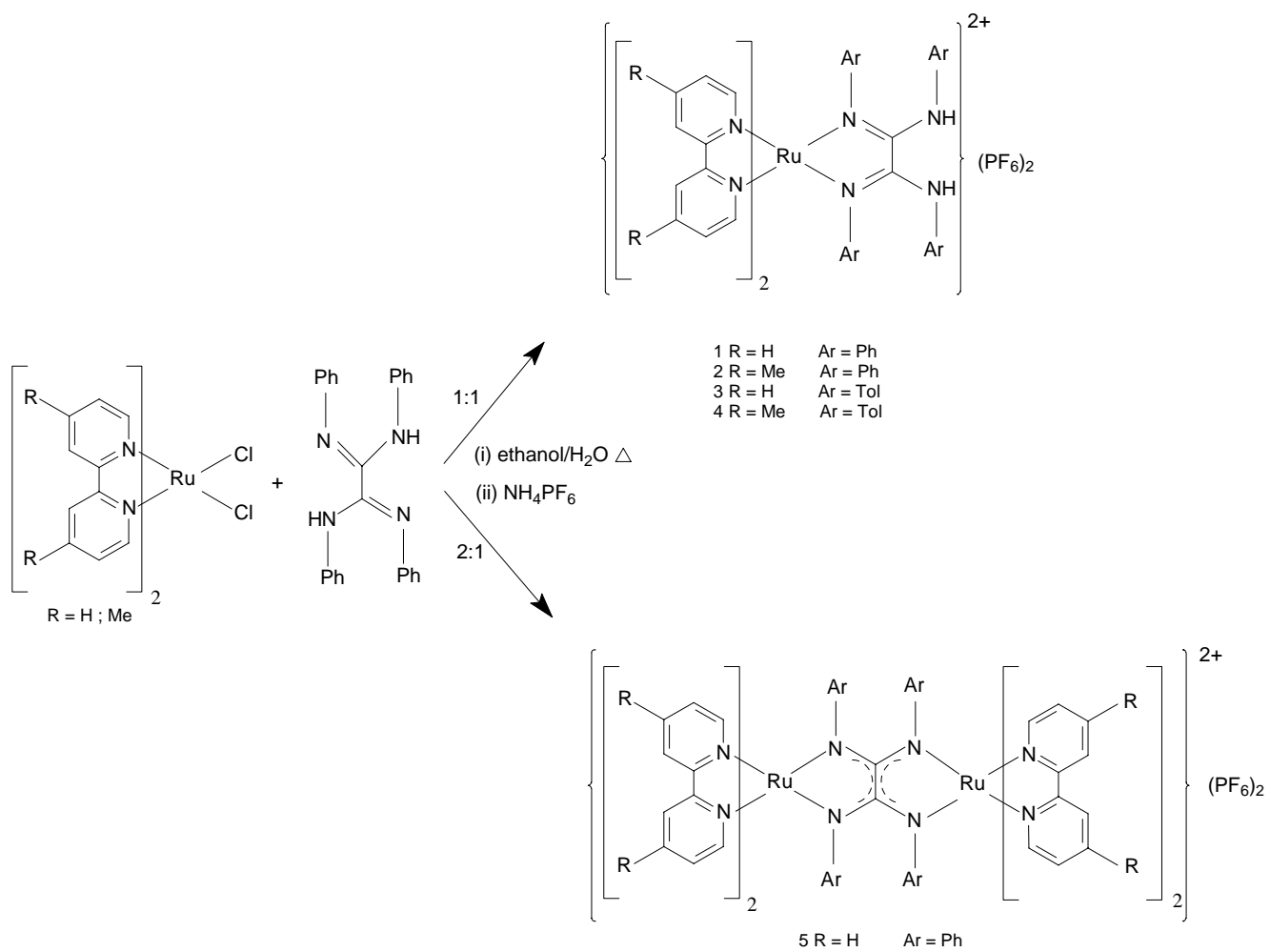


[Figure 3]

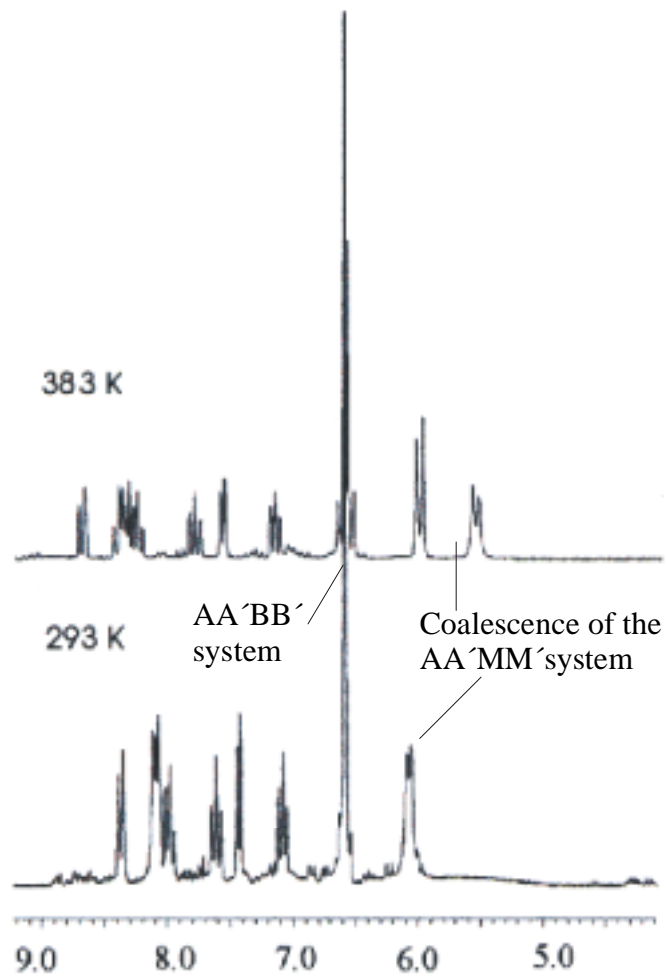


[Figure 4]

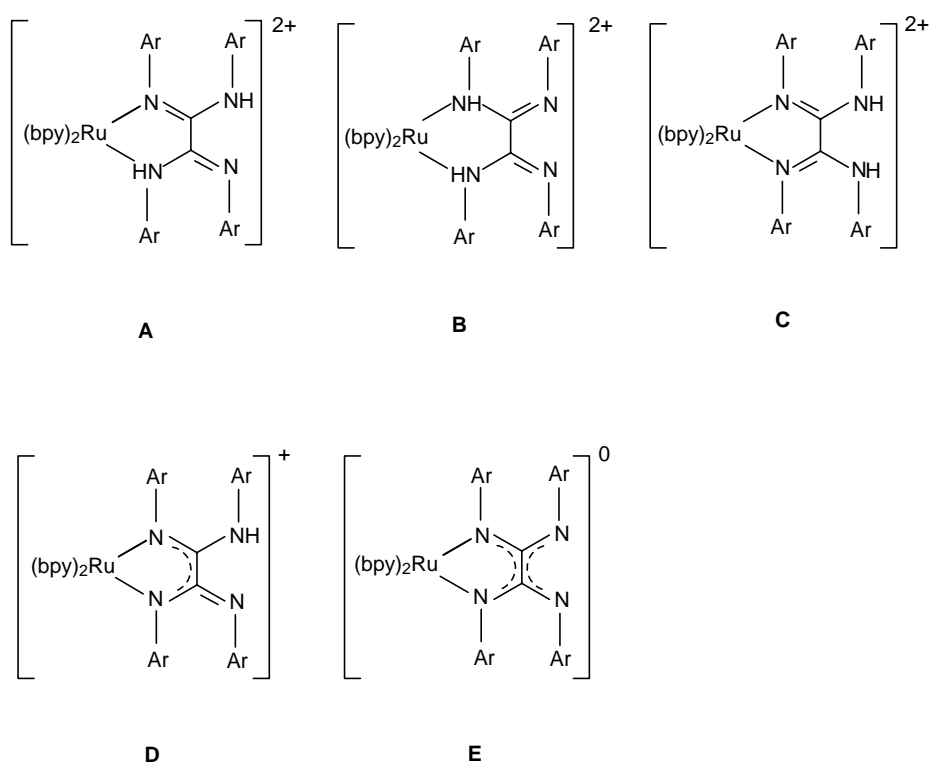


[Figure 5]

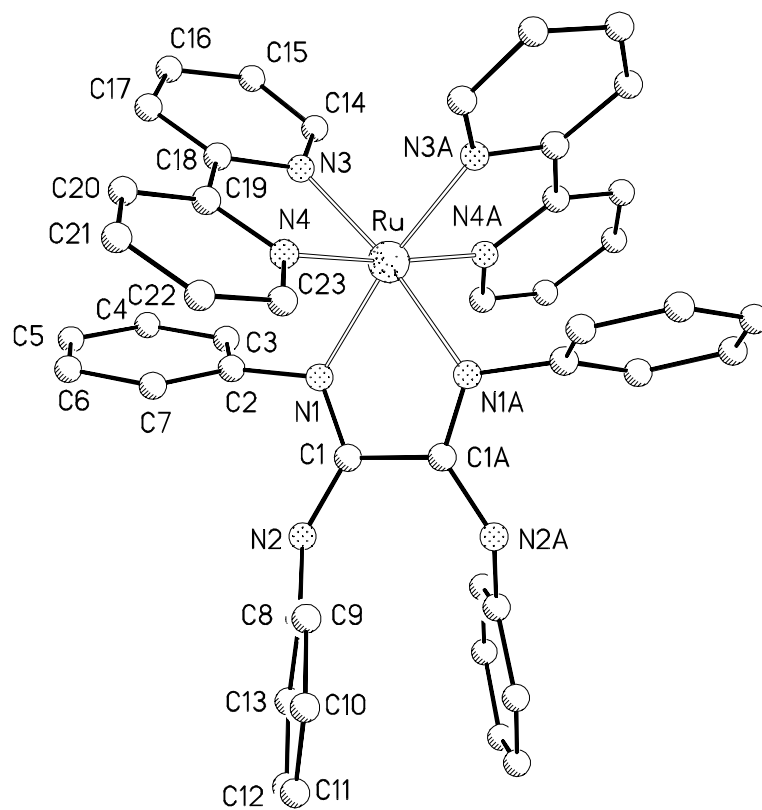


[Figure 6]

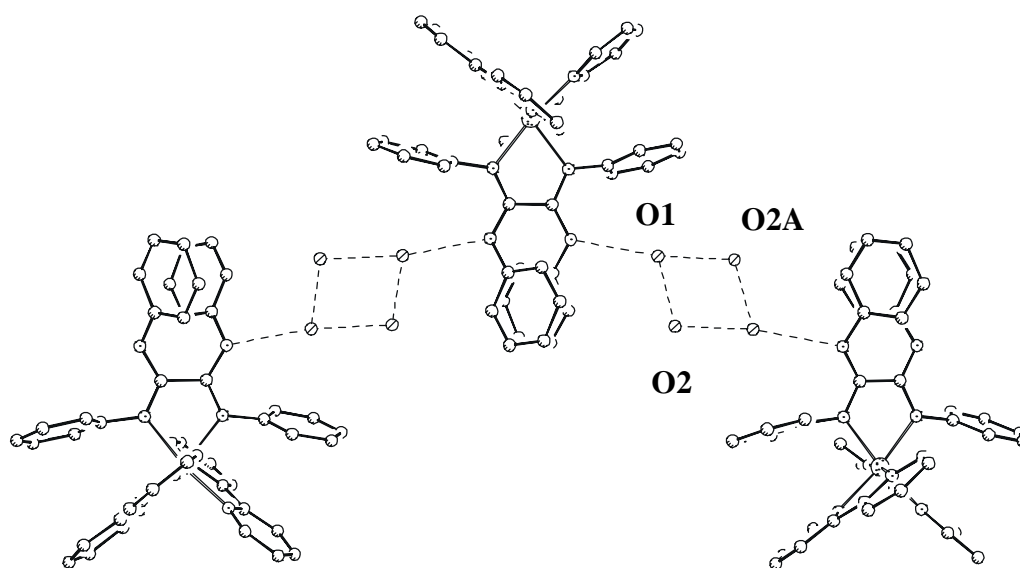


[Figure 7]

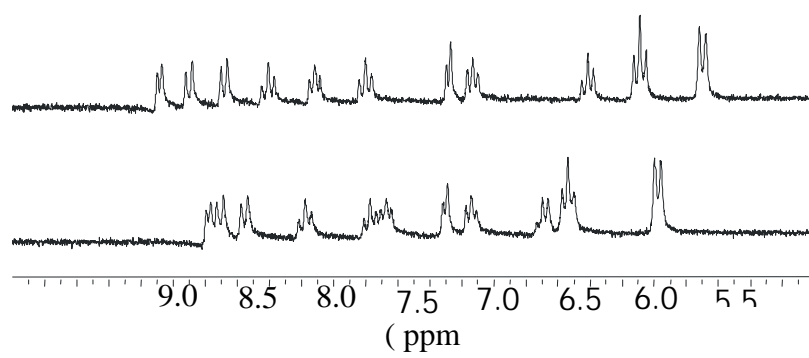


[Figure 8]

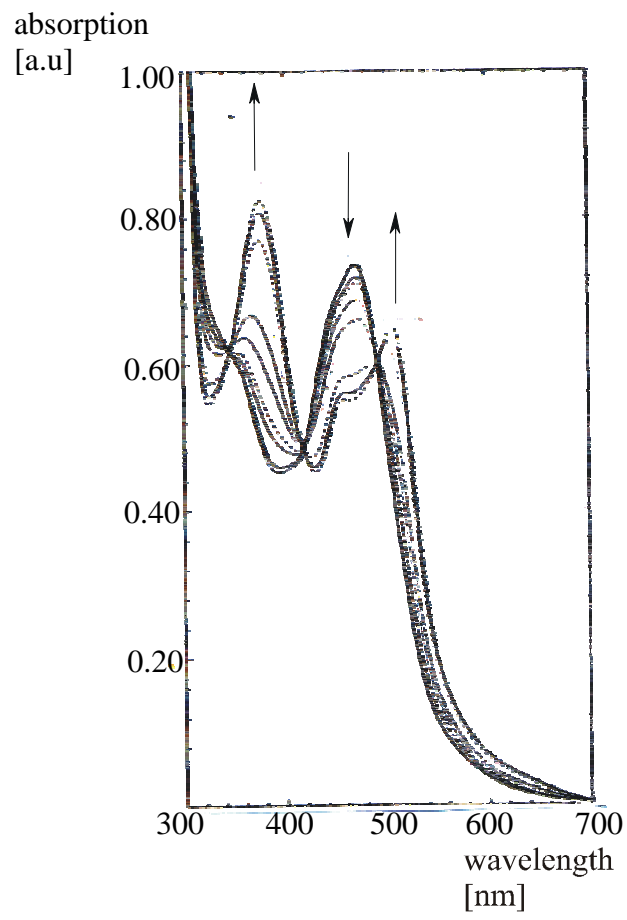
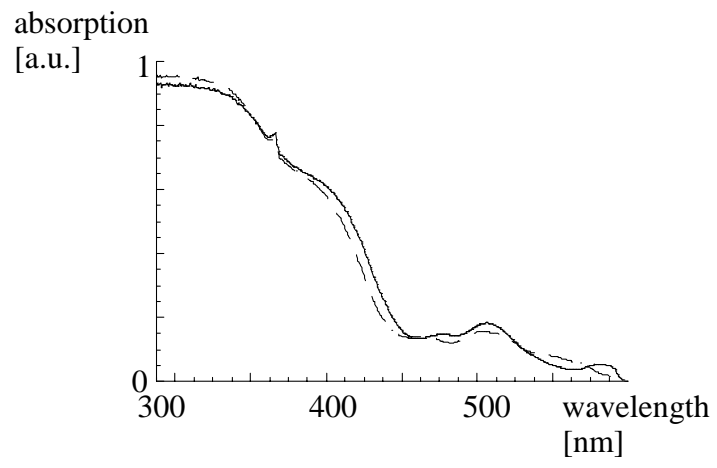
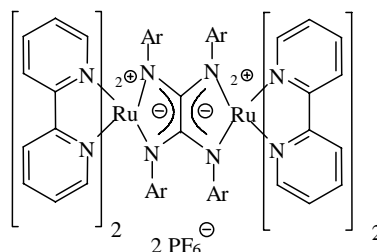


[Figure 9]



Pictogramm (for the list of content)

Novel polypyridyl Ruthenium(II) complexes containing oxalamidines as ligands were prepared and fully characterized. Their acid base and electrochemical properties are discussed. The dimeric complex could be separated in its diastereomers.



M. Ruben, S. Rau, A. Skirl, K. Krause, H. Görls, D. Walther, J. G. Vos